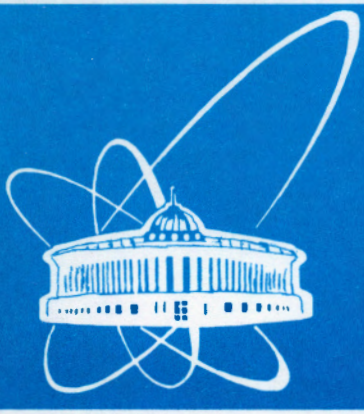

СООБЩЕНИЯ
ОБЪЕДИНЕННОГО
ИНСТИТУТА
ЯДЕРНЫХ
ИССЛЕДОВАНИЙ

Дубна

99-342

E13-99-342

A.Ya.Astakhov, Yu.A.Batusov, L.M.Soroko,
S.V.Tereshchenko, V.V.Tereshchenko

DARK-FIELD SCANNING CONFOCAL MICROSCOPE FOR VERTICAL PARTICLE TRACKS IN NUCLEAR EMULSION

1999

INTRODUCTION

The principle of the caustical meso-optical microscope for vertical particle tracks in the nuclear photoemulsion was explained in [1]. There were presented some non-traditional illuminating systems in this microscope. The results of the experiments performed with various setups, equivalent to the real microscope, were given.

The first variant of the meso-optical microscope for selective observation of the vertical particle tracks was explained in [2]. The scanning operation along depth coordinate was completely eliminated in this microscope. In the subsequent system [3] the efficiency of the search of the vertical particle tracks was increased due to the new observation algorithm with simultaneous scanning operations over ~100 fields of view.

To suppress the noise induced by the light diffraction side-lobes, a confocal meso-optical microscope has been proposed [4]. In this microscope the meso-optical condensor has been used. The illuminating region had the form of the narrow "fens" oriented parallel to the optical axis of the system. The searching and the measuring algorithms in this microscope are based on the principle of the reconstructed tomography [5]. The output efficiency of this meso-optical microscope for selective observation of the vertical particle tracks was estimated to be 10^2 times higher than in the traditional optical microscope with 3D-scanning operations.

To ameliorate the signal-to-noise ratio of the earlier microscope there were proposed in [5,6] some new variants of the meso-optical condensor [1]. The period of the interference fringes in the illuminating region was changing along depth coordinate. The confocal variants of this microscope were described, and the results of the experiments performed with various equivalent setups were given [1].

In this paper we explain the principle of the dark-field scanning confocal (DAFISCON) microscope for selective observation of the vertical particle tracks in nuclear emulsion. The construction of the DAFISCON microscope, built on the basis of the 2D measurement microscope, is described. We present the results of the experimental testing of the DAFISCON microscope accomplished at high density of the vertical particle tracks. The width, the depth and the length of the illuminating volume are estimated. The 2D plot and the 1D plot of the detected vertical particle tracks are presented. The real spatial resolution of our microscope provided by the low aperture objective, x8/0.16, can be increased by suing the objective with higher aperture.

ILLUMINATING SYSTEM

The principle of the illuminating system of our confocal microscope is given in Fig. 1. The collimated light beam from laser 1 goes through the positive lens 2 and then through cylindrical lens 3. The narrow illuminating region is projected on the plane 5 by means of the microscope objective 4.

To observe in detail the structure of the cylindrical illuminating system we have

used the geometry of the setup shown in Fig. 2. Cylindrical lens L_C with focus length F=50 mm is illuminated by the collimated light beam. The monochromatic interference pattern of the caustic produced near the focus of the lens L_C was detected on the photoplate HPh which provides the spatial resolution of the order of 1 000 lines per mm. The photoplate HPh was inclined at some angle θ_Z with respect to the light beam axis. The microscopic structure of this interference pattern is shown in Fig. 3, where the focus part of this pattern is marked by F_{focus} and the system of indices C_i (i = 1,2, ..., 6, ..., 10, 12, 14, 16) marks the position of the interference pattern in which the number of the secondary internal maxima inside the caustical structure is equal to "i".

The longitudinal position coordinates Z_i of the interference pattern marked by C_i is the linear function of $\sqrt{C_i}$ (Fig. 4). We used only two parts of the whole interference pattern: the focus region F and the region with only one secondary maximum, C_1. The microscopic structure of these two regions is shown in Fig.5.

WHAT DO WE DETECT IN DAFISCON MICROSCOPE?

The photoelectrical signal detected by CCD attached to our microscope differs from the photoelectrical signal in the pure confocal microscope. This difference follows from the fact that our microscope is only the semi-confocal one as the observing part of our microscope consists of the traditional imaging microscopic objective. The latter has the restricted depth of focus which is much smaller than the depth of the caustical illuminating region, and which is also smaller than the depth of the nuclear emulsion layer h. To detect the signal in focus from the whole depth h we need meso-optical cylindrical objective described in Fig. 6 in [1].

The real situation in our microscope is shown in Fig. 6, where ΔZ is the depth of focus of the imaging objective, θ is the inclination angle of the "vertical particle track", and Δ is the width of the illuminating region inside the nuclear emulsion layer. We can change the position of the focus region of the depth $\Delta Z < h$ by changing the position of the imaging objective, along the vertical particle track, going from the point $0'$ on the front surface of the layer down to the point A on the bottom surface of the nuclear emulsion layer.

CONSTRUCTION

Complete scheme of the DAFISCON microscope designed for selective observation of the vertical particle tracks is shown in Fig. 7, where 1 — laser, 2 — plane mirror, 3 — positive lens, 4 — plane mirror, 5 — cylindrical lens, 6 — nuclear emulsion layer, 7 — microscopic objective, 8 — moving X,Y stage with 2D position indicator, 9 — CCD pick-up system, 10 — CCD monitor system, 11 — rotating system for changing the angle θ between the vertical particle track and the optical axis of the

whole system, 12 — indicator of the angular orientation of the vertical particle track. The construction of the dark-field system is shown below: θ — objective, S — dark screen, NE — nuclear emulsion.

The collimated laser beam from laser 1 is reflected from the plane mirror 2 and is directed onto the positive lens 3. The divergent illuminating light beam is converted into the one-dimensional picture by the cylindrical lens 5.

Only a narrow region of the nuclear emulsion layer is illuminated by this system. The transverse width of this region is defined by the position of the nuclear emulsion layer with respect to the focus region. In the position F the width is equal to 6 μm, and in the position C_1 the width of the central lobe is equal to 4 μm (see Fig. 5).

The back view of our microscope is given in Fig. 8, where we see laser 1, plane mirror 2, positive lens 3, the driving part of the rotating system 11, microscopic objective 7, CCD system 9, and also the white light illuminator 13 of the marker grid on the front surface of the nuclear emulsion layer 6. We see also the diffraction grating 14 of the X, Y position indicator of the moving stage 8.

The side view of our microscope is shown in Fig. 9, where we see the driving part of the rotating system 11, microscopic objective 7, illuminator 13, CCD pick-up system 9 and CCD monitor 10.

The top view of our microscope is shown in Fig. 10, where we see the nuclear emulsion layer 6, microscopic objective 7, illuminator 13, CCD pick-up system 9 and the driving part of the rotating system 11.

EXPERIMENTS

The real "vertical" particle track never goes well along optical axis of the microscope. Going from the input point $0'$ to the output point "A" on the bottom of the nuclear emulsion layer of the depth h, the track produces a projection vector R_θ $(\Delta x, \Delta y)$ (Fig. 11).

To estimate the performance parameters of our microscope we have chosen a small part of the nuclear emulsion which contains 16 vertical particle tracks in the quadratic area 43×43 μm^2 (Fig. 12). The vector R_θ, shown in Fig. 11, is presented by the arrow. The positions of the vectors R_θ $(\Delta x, \Delta y)$ for all 16 particle tracks are shown in Fig. 13, with appex "ap". The average $\overline{R_\theta} \approx 15$ μm, and $\overline{\theta} \approx 4.5°$.

The signals on the CCD monitor screen for some position of the moving stage 8 are presented in Fig. 14 for the illuminating region F, and in Fig. 15 for the illuminating region C_1. In the latter case we use information only in the central internal maximum.

The digital 2D signals along the working strip of the width 20 pixels for Fig. 14 are presented in Fig. 16 over the partial longitudinal length 53 pixels. The xy-coordinate system on the top of the Fig. 16 refers to the input 2D CCD image shown on the narrow dark-field strip above. The total length of the 2D CCD image is equal to 629 pixels along X-axis shown below the narrow dark-field strip. The total number of the candidate maxima of the vertical particle tracks estimated by visual inspection is equal to 51. From these data we have constructed the one-dimensional digital

signal $\sum(i)$ by summing along transversal coordinate, and then by averaging of thus constructed signals in two adjacent points along the illuminating region. Thus we have get the data shown in Fig. 17 for F illuminating region.

We see that 1D digital signals $I(X)$ reveal well pronounced 48 maxima of the width $\Gamma_{1/2}$ at half the maximum. The distribution of the vertical particle tracks at different $\Gamma_{1/2}$ is shown in Fig. 18. We see two groups of the vertical particle tracks, one with average $\Gamma_{1/2}^{AV} \approx 8$ pixels.

The distribution of the vertical particle tracks at different amplitude A of the maximum is shown in Fig. 19. This distribution can be approximated with constant value from $A = 0$ to $A = 600$ units.

The difference between number of maxima $N_{2D} \approx 51$, estimated by visual inspection, and the number of the maxima $N_{1D} \approx 48$, estimated by inspection of the 1D-spectra presented in Fig. 17, can be partially explained by the superimposition under projection of two maxima in 2D plot onto one maximum in 1D plot.

The distribution of the vertical particle tracks at peak amplitude A and width $\Gamma_{1/2}$ is shown in Fig.20. The pronounced correlation between A and $\Gamma_{1/2}$ is observed.

CONCLUSIONS

1. The principle of the DAFISCON microscope for selective observation of the vertical particle tracks in nuclear emulsion is explained.

2. The construction of the DAFISCON microscope, built on the basis of the 2D measurement microscope, is described.

3. The results of the experimental testing of the DAFISCON microscope accomplished at high density of the vertical particle tracks are presented.

4. The dark-field imaging of the particle tracks in nuclear emulsion in our microscope provides bright signals on the dark background and facilitates the operation of the CCD plus computer system.

5. The depth of the illuminating volume is equal to 200 μm and the depth scanning in our microscope is absent.

6. The width of the illuminating volume is equal to $\approx 6\,\mu$m, so the transversal step of the area scanning operation can be taken to $\approx 4 \div 5\,\mu$m.

7. The length of the illuminating volume is equal to 250 μm, so the longitudinal dimension of the area scanned simultaneously is equal to 250 μm.

8. The XY-dimensions of the pickes produced by the vertical particle tracks on the 2D plots are equal to 5 × 5 pixels, and about 6 pixels on the 1D plots.

9. The real spatial resolution of our microscope provided by the low aperture objective, x8.0/0.16, can be increased by using of the high aperture objective.

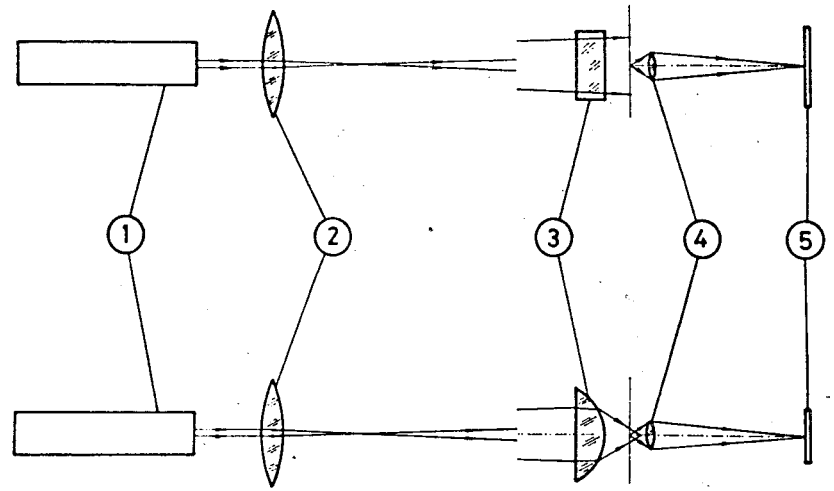

Fig.1. The principle of the illuminating system of the DAFISCON microscope

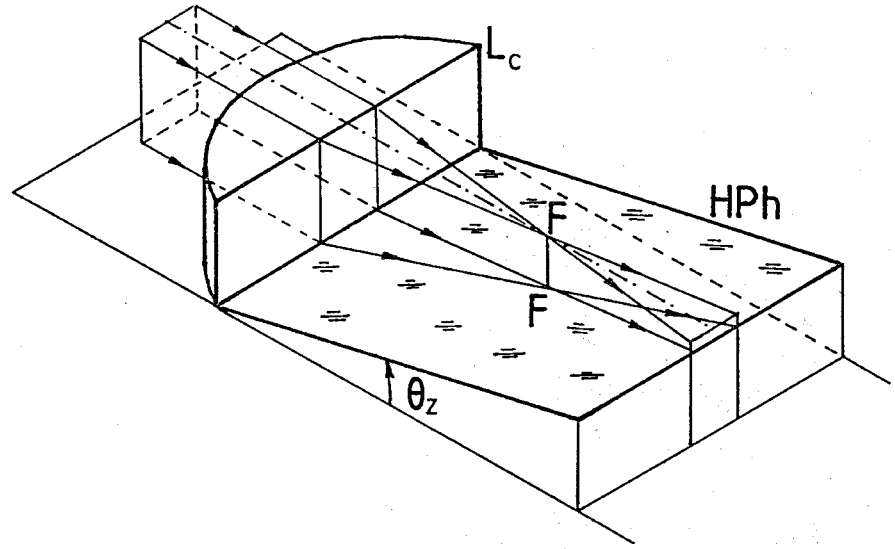

Fig.2. The setup for detection of the microstructure of the internal caustic picture: L_c — cylindrical lens, HPh — photoplate, F — position of the focus, θ_z is the angle between the photoplate HPh and the light beam axis

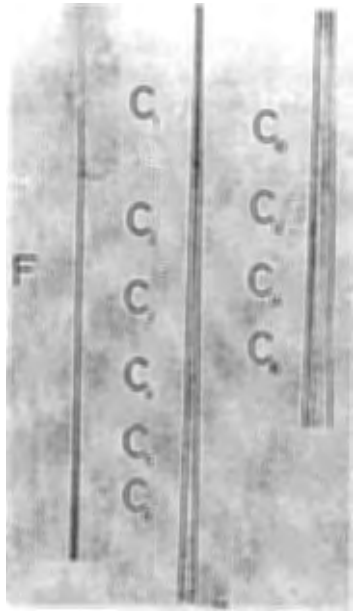

Fig.3. The microscopic structure of the internal caustic picture (see text)

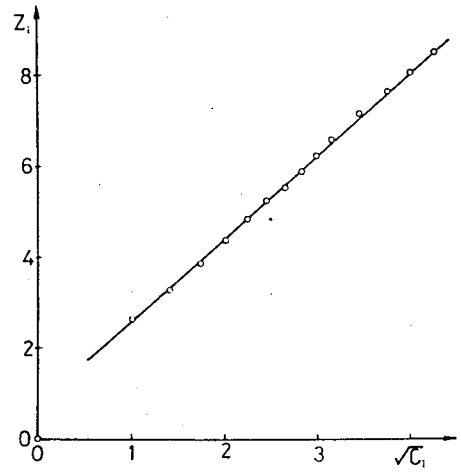

Fig.4. The dependence between number of the internal maxima C_i of the microscopic structure of the internal caustic picture and the longitudinal coordinate Z_i of the corresponding maxima

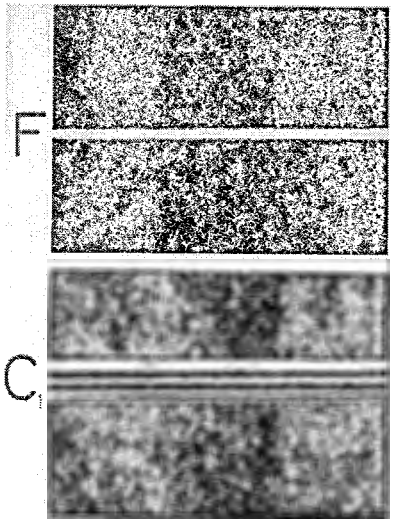

Fig.5. The structure of the caustic pictures in F and in C_1 positions

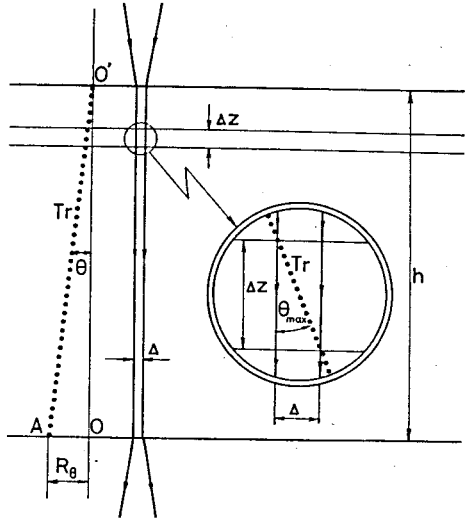

Fig.6. The position of the «vertical» particle track in nuclear emulsion layer (see text)

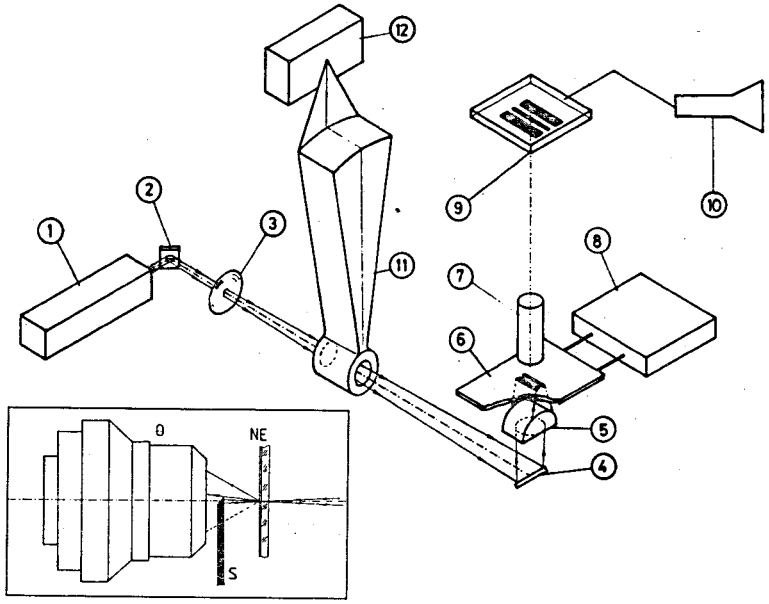

Fig.7. The complete scheme of the DAFISCON microscope construction (above). The construction of the dark field system: O — objective, S — dark screen, NE — nuclear emulsion

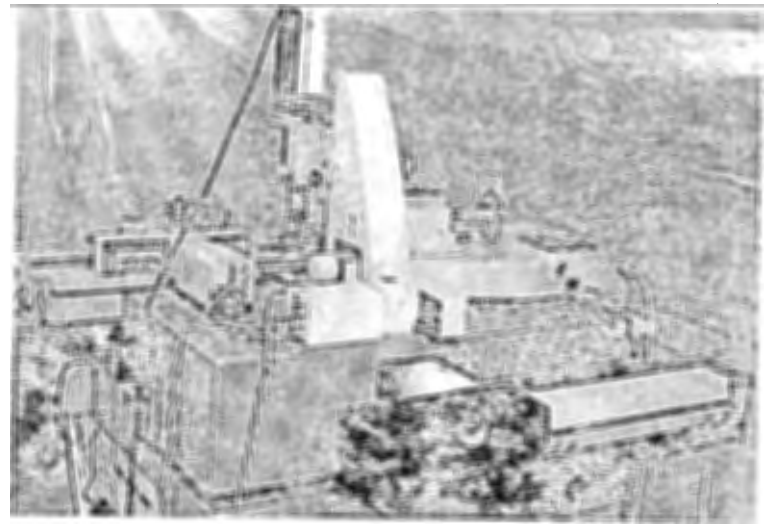

Fig.8. The back view of the DAFISCON microscope

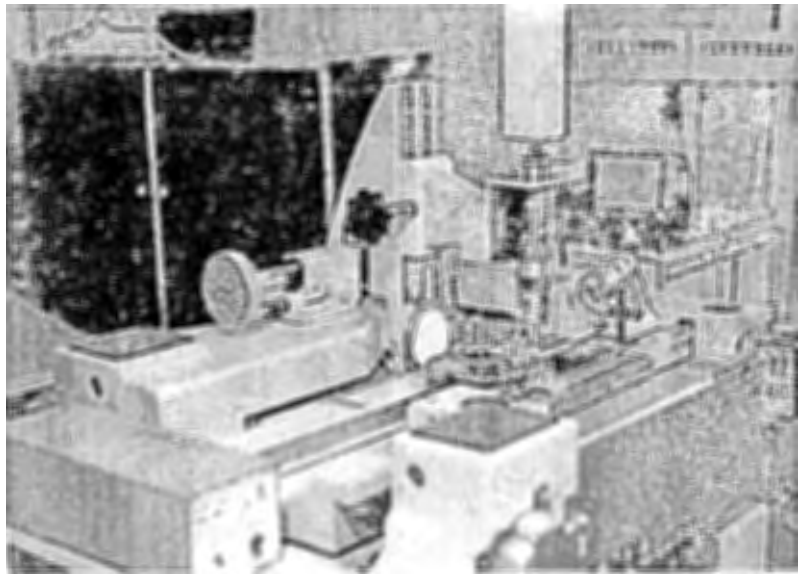

Fig.9. The side view of the DAFISCON microscope

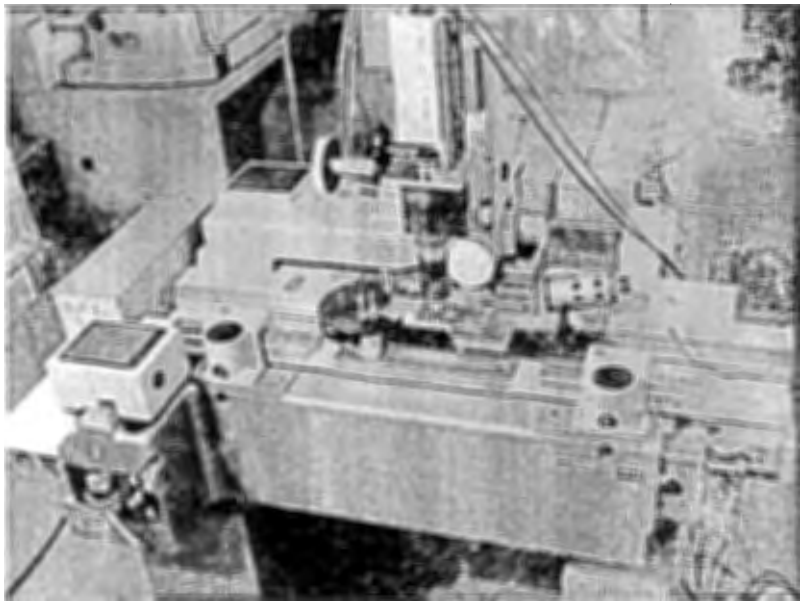

Fig.10. The top view of the DAFISCON microscope

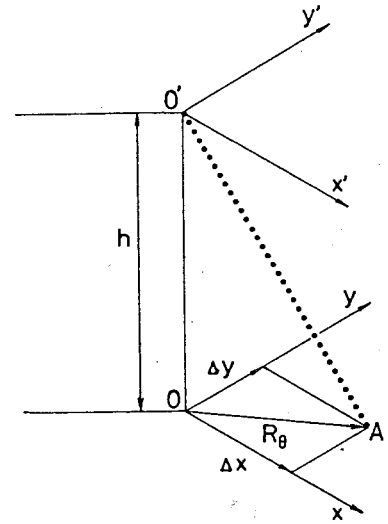

Fig.11. The position of the real «vertical» particle track in the nuclear emulsion layer

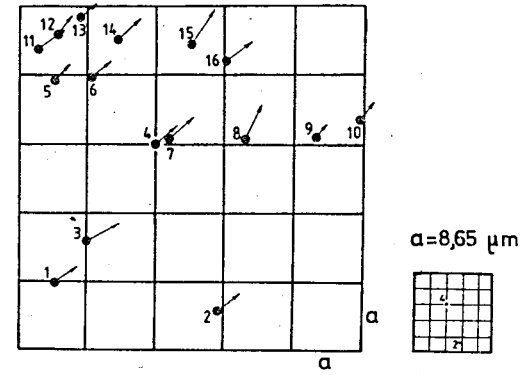

Fig.12. The quadratic area with 16 vertical particle tracks, 1, ..., 16

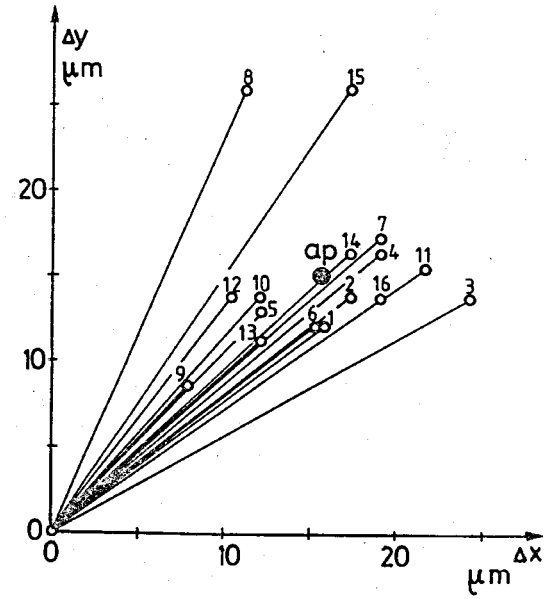

Fig.13. The distribution of the R_θ-vectors

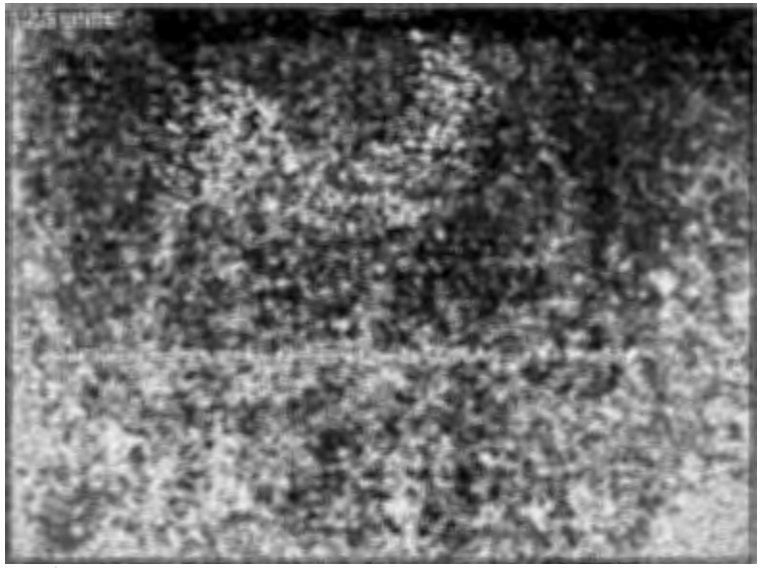

Fig.14. The view of the signals in the DAFISCON microscope on the CCD monitor screen for F illuminating regions

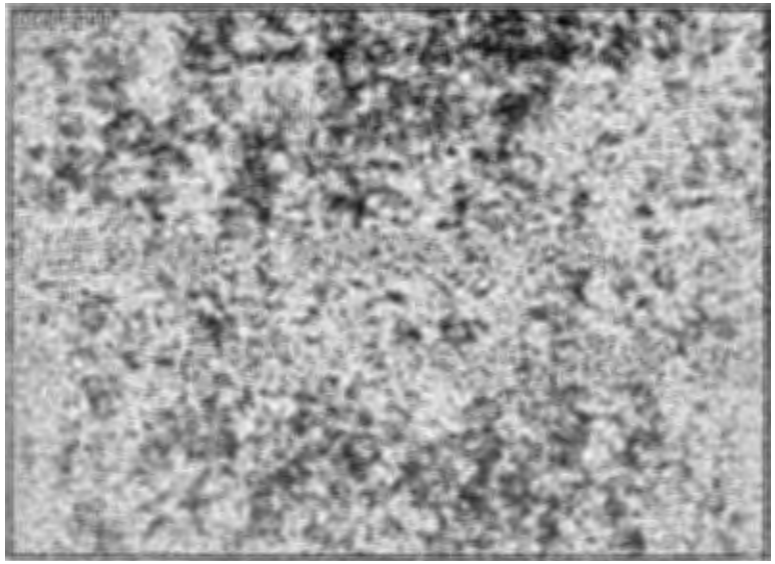

Fig.15. The view of the signals in the DAFISCON microscope on the CCD monitor screen for C_1 illuminating region

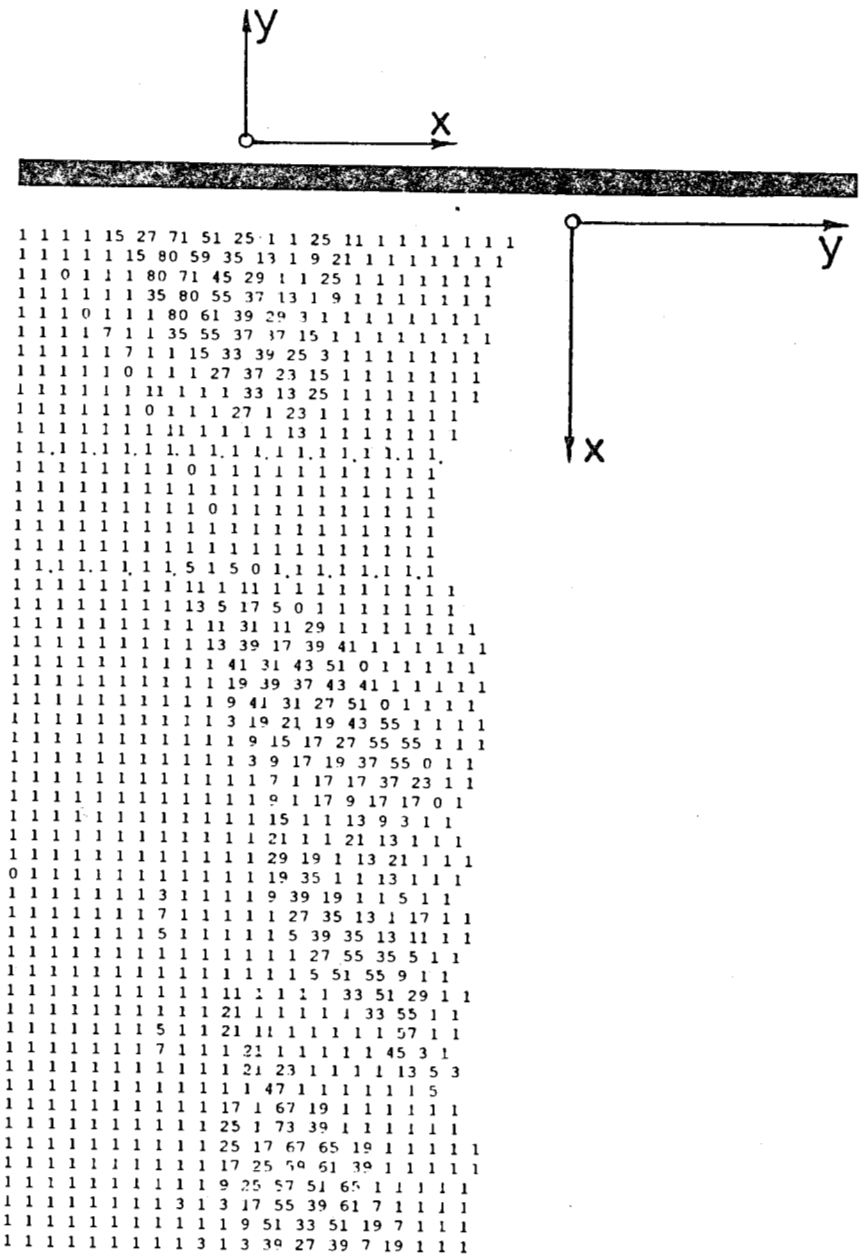

Fig.16. 2D plot of the CCD signals in the DAFISCON microscope for F illuminating region

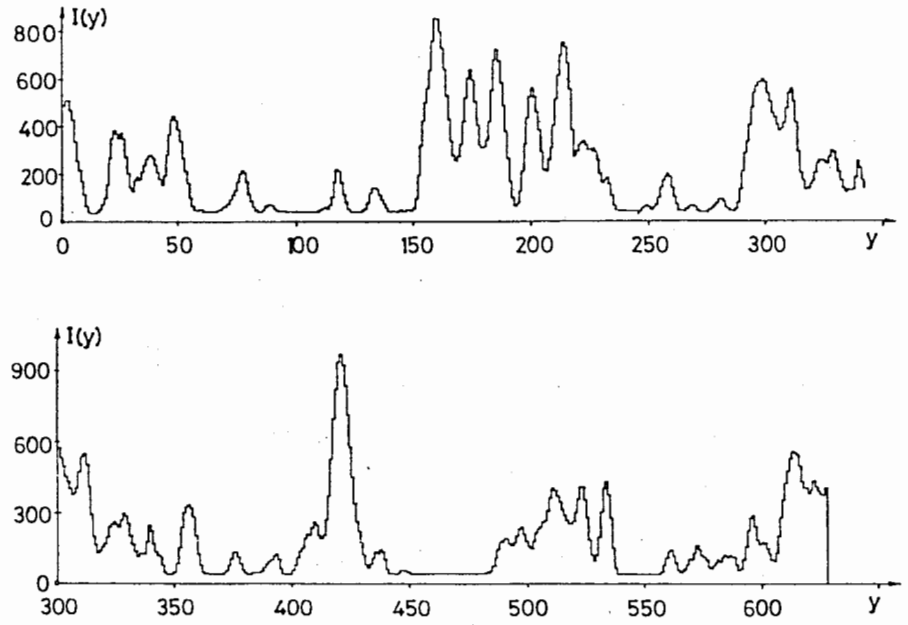

Fig.17. 1D plot of the CCD signals in the DAFISCON microscope for F illuminating region

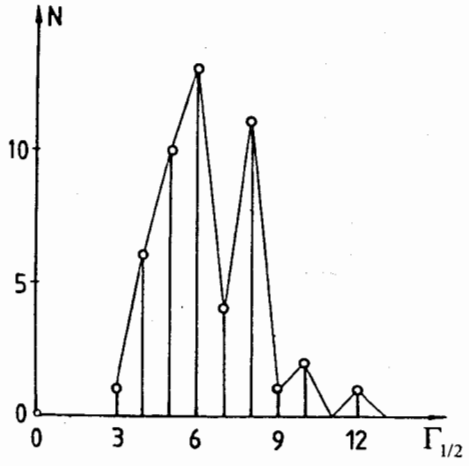

Fig.18. The distribution of the detected vertical particle tracks versus maximum width $\Gamma_{1/2}$

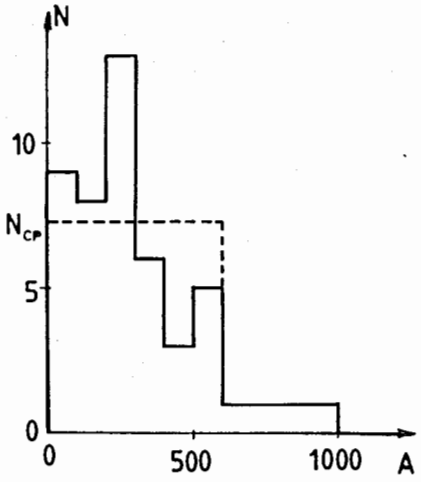

Fig.19. N versus maximum amplitude A

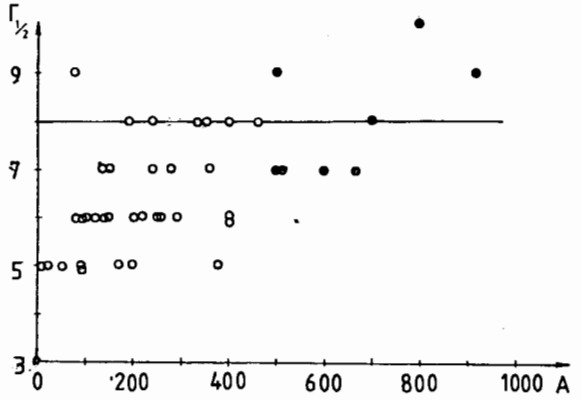

Fig.20. The maximum width $\Gamma_{1/2}$ versus maximum amplitude A

REFERENCES

1. Soroko L.M. — JINR Commun. E13-95-545, 1995, Dubna.
2. Soroko L.M. — JINR Commun. P13-87-576, 1987, Dubna.
3. Soroko L.M. — USSR Patent No 1.234.796, Bull. No 20, p.203, 1986.
4. Soroko L.M. — USSR Patent No 1.183.934, Bull. No 37, p.191, 1985.
5. Soroko L.M. — Exper. Techn. der Physik, (1990) v. 38, 5/6, p.411.
6. Soroko L.M. — USSR Patent No 1.273.861, Bull. No 44, p.180, 1986.
7. Soroko L.M. — JINR Commun. E13-95-546, 1995, Dubna.

Received by Publishing Department
on December 28, 1999.